Environmental Science: Atmospheres

ROYAL SOCIETY OF CHEMISTRY

PAPER

View Article Online
View Journal | View Issue



Cite this: *Environ. Sci.: Atmos.*, 2023, **3**, 672

# An unexpected feasible route for the formation of organosulfates by the gas phase reaction of sulfuric acid with acetaldehyde catalyzed by dimethylamine in the atmosphere†

Ju-Rui Yang,[a] Ai Liu[b] and Bo Long *[ab]

Received 20th November 2022
Accepted 2nd February 2023

DOI: 10.1039/d2ea00159d

rsc.li/esatmospheres

An understanding of the formation of organosulfates is required for elucidating the formation of secondary organic aerosols in atmosphere. Herein, we report a new feasible reaction pathway for the formation of organosulfates in the reaction of sulfuric acid ($H_2SO_4$) with acetaldehyde ($CH_3CHO$) catalyzed by dimethylamine ($(CH_3)_2NH$) using quantum chemical methods and reaction rate theory. We found that dimethylamine has a strong catalytic effect in the $CH_3CHO + H_2SO_4 + (CH_3)_2NH$ reaction because the energy barriers of the $CH_3CHO + H_2SO_4 + (CH_3)_2NH$ reaction are reduced by 18.28–23.08 kcal mol$^{-1}$ as compared to the $CH_3CHO + H_2SO_4$ reaction. The calculated results show that the $CH_3CHO + H_2SO_4 + (CH_3)_2NH$ reaction can compete well with the traditional sink for $CH_3CHO$ by hydroxyl radicals (OH), when the OH, $H_2SO_4$, and $(CH_3)_2NH$ concentrations are $10^4$ molecules per cm$^3$ during the night and $1.0 \times 10^6$ and $3.2 \times 10^9$ molecules per cm$^3$ at below 240 K, respectively. The calculated results also show that the $CH_3CHO + H_2SO_4 + (CH_3)_2NH$ reaction makes a limited contribution to the sink for sulfuric acid in the atmosphere. The present findings provide a new insight into the generation of organosulfates, which could be extended to other aldehydes with sulfuric acid catalyzed by amines in the atmosphere.

### Environmental significance

Organosulfates are key components in secondary organic aerosols. This study presents a new feasible route for the formation of organosulfates *via* the gas phase reactions of acetaldehyde with sulfuric acid catalyzed by dimethylamine. This mechanistic route could be extended to the reactions of other aldehydes with sulfuric acid catalyzed by amines in the atmosphere. However, organosulfates are often obtained by heterogeneous processes. Our findings also show that the $CH_3CHO + H_2SO_4 + (CH_3)_2NH$ reaction can make an important contribution to the sink for acetaldehyde during the night at low temperatures. This study is of great significance for the accurate evaluation of the atmospheric environmental effects of $CH_3CHO$, particularly, air quality and atmospheric modeling and policies.

## 1. Introduction

Secondary organic aerosols (SOAs) are formed by the atmospheric oxidation of volatile organic compounds (VOCs),[1–8] which have important effects on the climate and environment, human health, and cloud condensation nuclei (CCN).[2,9–17] Although there are extensive studies on secondary organic aerosols, the formation process of secondary organic aerosols is

[a]*Department of Physics, Guizhou University, Guiyang 550025, China. E-mail: wwwltcommon@sina.com*

[b]*School of Materials Science and Engineering, Guizhou Minzu University, Guiyang, 550025, China*

† Electronic supplementary information (ESI) available: The $T_1$ diagnostic values for all the species as listed in Table S1; the calculated relative energies with zero-point vibrational correction of the dimer complexes as listed in Table S2; the calculated equilibrium constants and the concentration of the dimer complexes when the $[(CH_3)_2NH] = 3.2 \times 10^9$, $[H_2SO_4] = 4 \times 10^8$, $[CH_3CHO] = 1.12 \times 10^{12}$ molecule per cm$^3$ for the $H_2SO_4 + (CH_3)_2NH + CH_3CHO$ in the temperature range of 200–298 K as listed in Table S3; the rate constants of the $CH_3CHO + H_2SO_4$ reaction as listed in Table S4; the rate ratio of each reaction as listed in Table S5; the rate ratio of the $v_1/v_{CH_3CHO+OH}$ at different OH concentrations in the temperature range of 200–298 K ($[(CH_3)_2NH] = 3.2 \times 10^9$, $[H_2SO_4] = 10^6$, $10^7$, $4.0 \times 10^8$ and $5.1 \times 10^9$ molecule per cm$^3$ respectively) as listed in Tables S6–S9; the rate ratio of the $v_1/v_{H_2SO_4+OH}$ at different OH concentrations in the temperature range of 200–298 K($[(CH_3)_2NH] = 3.2 \times 10^9$, $[CH_3CHO] = 1.12 \times 10^{12}$ molecule per cm$^3$ respectively) as listed in Table S10; calculated atmospheric lifetime of $H_2SO_4$ ($[(CH_3)_2NH] = 3.2 \times 10^9$, $[CH_3CHO] = 2.46 \times 10^9$ and $1.12 \times 10^{12}$ molecule per cm$^3$ respectively) as listed in Tables S11 and S12; molecular coordinates and molecular frequencies as listed in Table S13; Gibbs free energy reaction profile of $CH_3CHO + H_2SO_4 + (CH_3)_2NH$ reaction at 298 K as listed in Fig. S1; relative energies with zero point correction for the $CH_3CHO + H_2SO_4$ reaction at 0 K as listed in Fig. S2; relative energies with zero point correction for $CH_3CHO + H_2SO_4 + (CH_3)_2NH$ reaction as listed in Fig. S3; selected geometrical parameters as shown in Fig. S4; intrinsic reaction coordinate results of TS1A, TS1B, TS1C, TS1D, TS1E and TS1F as listed in Fig. S5–S10. See DOI: https://doi.org/10.1039/d2ea00159d

still not completely clear because their formation is significantly influenced by many factors such as the complex atmospheric oxidation processes of VOCs and different sources of atmospheric particles.[2,9,18,19]

The formation of secondary organic aerosols occurs by atmospheric nucleation,[20] which is determined by the formation and decomposition of molecular clusters of different sizes and chemical compositions.[21] Previous studies have shown that sulfuric acid is the most common nucleating precursor and dimethylamine is an important component of atmospheric aerosol precursors in acid-base cluster reactions.[22–25] The strong interactions between dimethylamine and sulfuric acid can effectively form clusters,[26–29] which further contribute to the formation of secondary organic aerosols.[27,28,30]

Acetaldehyde ($CH_3CHO$) is an important aldehyde with atmospheric concentrations of about 15.9 ppb and 45.60 ppb in major urban areas of China and Brazil, respectively.[31,32] $CH_3CHO$ has serious impacts on the air environment,[33–36] and is emitted from anthropogenic and natural sources.[32,35,37–41] Additionally, the photochemical degradation of VOCs has been considered to be the main source of acetaldehyde in the atmosphere.[31,37,42] Previous studies have shown that acetaldehyde makes an important contribution to the formation of secondary organic aerosols.[36,41] Organosulfates are formed *via* the heterogeneous reaction process of aldehydes as reported in the literature.[43,44] However, the formation of organosulfates by acetaldehyde has not been reported in the gas phase of the atmosphere.

$$CH_3CHO + H_2SO_4 + (CH_3)_2NH \rightarrow CH_3CHO + H_2SO_4\cdots(CH_3)_2NH \rightarrow CH_3HC(OH)OSO_3H + (CH_3)_2NH \quad (R1)$$

Herein, we have investigated the reaction of sulfuric acid with acetaldehyde catalyzed by dimethylamine in reaction (R1) using theoretical methods. We obtained the energy barriers and reaction rates of reaction (R1) to show the catalytic ability of dimethylamine. We propose a new mechanistic pathway for the formation of organosulfates *via* the homogeneous reaction process, whereas previous investigations considered the formation of organosulfates by heterogeneous reaction processes.[45] The present findings of this work not only provide a new source of organosulfates but are also likely to be applied in other aldehyde reactions with sulfuric acid catalyzed by dimethylamine.

## 2. Computational methods

In this article, all geometries and the corresponding frequencies of reactants, transition states, products, and complexes were optimized using the M06-2X[46] functional with the MG3S[47] basis set in the $CH_3CHO + H_2SO_4 + (CH_3)_2NH$ reaction. The reliability of the M06-2X functional and its wide application have been demonstrated in previous studies on the atmospheric reactions of sulfuric acid and sulfuric acid molecular clusters.[48–53] The calculated results of the corresponding frequencies of reactants, complexes, transition states, and products using M06-2X/MG3S suggest that all stable structures have positive frequencies, while the transition state has only one imaginary frequency. The stability of the density functional theory method has been tested by using the keyword (stable = opt).[54,55] Intrinsic reaction coordinate (IRC)[56,57] calculations were utilized to determine whether the transition state corresponds to the reactants and products.

To obtain the relative energies more reliably, we did single-point energy calculations for these stationary points in the present investigation. Based on previous studies, the accuracy of CCSD(T)-F12a/jun-cc-pV(T+d)Z calculation results can be approximated to CCSD(T)/CBS.[58,59] Therefore, we have used the CCSD(T)-F12a[60,61] theoretical method and the jun-cc-pV(T+d)Z[62] basis set to calculate the single-point energies to obtain reliable relative energies based on the optimization geometric structure of M06-2X/MG3S. The reliability of CCSD(T) has been confirmed by the $T_1$ diagnostic values of all species with the upper limit of 0.02 in the closed-shell systems.[63] The $T_1$ diagnostic values of all species in this article are below the upper limit of 0.02 (see Table S1†).

We calculated rate constants by using conventional transition state theory[64–66] with Eckart tunneling[67] for each reaction studied in this article. All electronic structure calculations were done using the Gaussian 16 (ref. 68) and Molpro 2019 (ref. 69) codes, while the rate constants were calculated using The Rate[70] code.

## 3. Results and discussion

The optimized geometries and calculated relative energies with zero-point vibrational correction for the reaction (R1) are shown in Fig. 1. Concerning the complexes and transition states reported here, we used the binding energies and energy barriers, which are equal to the relative energies obtained by CCSD(T)-F12a/jun-cc-pV(T+d)Z//M06-2X/MG3S, plus the relative zero-point vibrational correction by M06-2X/MG3S, respectively. The rate constants and equilibrium constants relative to the reaction (R1) are listed in Table 1. The relative Gibbs free energy for the reaction of acetaldehyde with sulfuric acid catalyzed by dimethylamine at 298 K is shown in Fig. S1.† We discuss the relative energies with zero-point vibrational correction based on CCSD(T)-F12a/jun-cc-pV(T+d)Z//M06-2X/MG3S calculated results unless otherwise stated.

### 3.1. The $CH_3CHO + H_2SO_4$ reaction catalyzed by $(CH_3)_2NH$

The reaction of acetaldehyde with sulfuric acid catalyzed by dimethylamine is shown in Fig. 1, where there are three molecular reaction systems. In trimolecular reaction systems, there are three different entrance channels, and the probability of the three molecules colliding simultaneously in the gas phase of the atmosphere is very low, which has been reported in the literature.[36,71–75] Therefore, when the three molecules $CH_3CHO$, $H_2SO_4$, and $(CH_3)_2NH$ first collide, two molecules of the three form a dimer, and then the dimer collides with the third molecule to form the ternary complex: $H_2SO_4\cdots(CH_3)_2NH + CH_3CHO$, $CH_3CHO\cdots H_2SO_4 + (CH_3)_2NH$, and $CH_3CHO\cdots(CH_3)_2NH + H_2SO_4$.

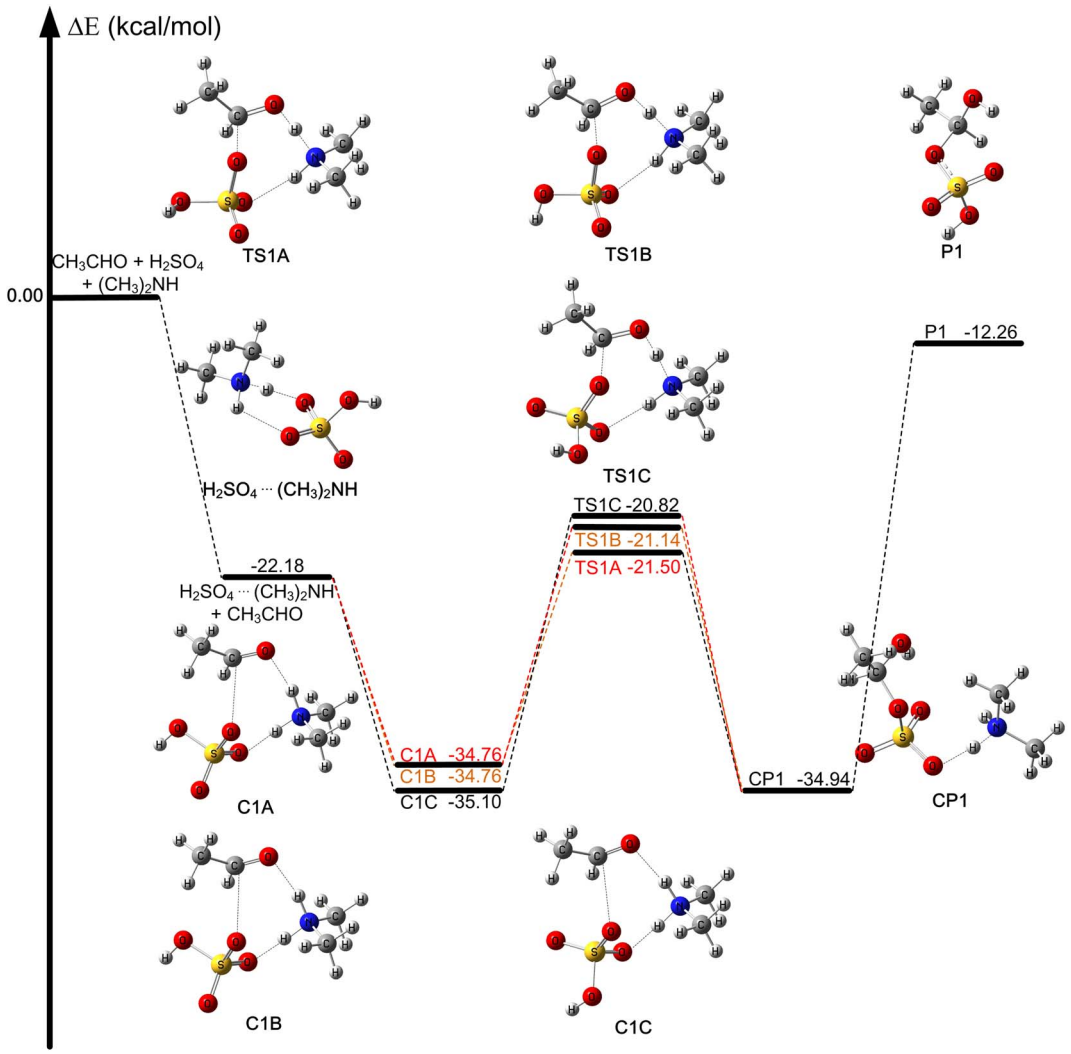


Fig. 1 Calculated relative energies with zero-point vibrational correction for the reaction $CH_3CHO + H_2SO_4 + (CH_3)_2NH \rightarrow CH_3HC(OH)OSO_3H + (CH_3)_2NH$ at the CCSD(T)-F12a/jun-cc-pV(T+d)Z//M06-2X/MG3S level (in kcal $mol^{-1}$).

Table 1 The calculated equilibrium constants ($K_{eq1}$, molecules per $cm^3$) and bimolecular rate constants ($k_1$, $cm^3$ per molecules per s) for the $H_2SO_4\cdots(CH_3)_2NH + CH_3CHO$ over the temperature range of 200–298 K

| | 200 K | 220 K | 240 K | 260 K | 280 K | 298 K |
|---|---|---|---|---|---|---|
| $K_{eq1}$ [a] | $2.33 \times 10^{-3}$ | $1.56 \times 10^{-5}$ | $2.43 \times 10^{-7}$ | $7.27 \times 10^{-9}$ | $3.63 \times 10^{-10}$ | $3.47 \times 10^{-11}$ |
| $k_1$ [b] | $1.55 \times 10^{-16}$ | $1.70 \times 10^{-16}$ | $1.90 \times 10^{-16}$ | $2.13 \times 10^{-16}$ | $2.40 \times 10^{-16}$ | $2.68 \times 10^{-16}$ |

[a] The equilibrium constants of the $H_2SO_4\cdots(CH_3)_2NH$ complex with respect to $H_2SO_4$ and $(CH_3)_2NH$. [b] The bimolecular rate constants of the $H_2SO_4\cdots(CH_3)_2NH + CH_3CHO$ reaction.

We compared the calculated binding energies of the dimer complexes with the values from previous investigations in the literature. The computed binding energy of $H_2SO_4\cdots(CH_3)_2NH$ (M1A) is −22.18 kcal $mol^{-1}$ (see Table S2†), which is consistent with the value of −21.99 kcal $mol^{-1}$ at the CCSD(T)/aug-cc-pVTZ//ωB97XD/6-311++(2d,2p) level.[76] The binding energy of $CH_3CHO\cdots H_2SO_4$ was computed to be −11.91 kcal $mol^{-1}$, which is slightly different from the value of $CH_3CHO\cdots H_2SO_4$ (−12.59 kcal $mol^{-1}$) at the CCSD(T)-F12a/cc-pVTZ-F12//M06-2X/MG3S level (see Table S2 and Fig. S2†). The calculated binding energy of $CH_3CHO\cdots(CH_3)_2NH$ (−3.43 kcal $mol^{-1}$) is consistent with the value of −3.42 kcal $mol^{-1}$ calculated by the CCSD(T)-F12a/VTZ-F12//M06-2X/6-311++G(d,p).[36] Because the binding energies of the binary complexes in the entrance channel were obtained using different theoretical methods, they do not exactly match the values in the literature.[77] However, the differences are still small (around 0.5 kcal $mol^{-1}$).

The binding energy of $H_2SO_4\cdots(CH_3)_2NH$ ($-22.18$ kcal mol$^{-1}$) is much lower than those of $CH_3CHO\cdots H_2SO_4$ ($-11.91$ kcal mol$^{-1}$) and $CH_3CHO\cdots(CH_3)_2NH$ ($-3.43$ kcal mol$^{-1}$); this resulted in the equilibrium constant of $H_2SO_4\cdots(CH_3)_2NH$ being much larger than those of $CH_3CHO\cdots H_2SO_4$ and $CH_3CHO\cdots(CH_3)_2NH$ in Table S3.† For example, the equilibrium constant of $H_2SO_4\cdots(CH_3)_2NH$ is at least $10^6$ and $10^{12}$ larger than those of $CH_3CHO\cdots H_2SO_4$ and $CH_3CHO\cdots(CH_3)_2NH$ at 298 K, respectively (see Table S3†). A larger equilibrium constant of the complex leads to a higher concentration in the atmosphere. For example, when the concentrations of $CH_3CHO$,[32,34] $H_2SO_4$,[78] and $(CH_3)_2NH$[79] are $1.12 \times 10^{12}$, $4.0 \times 10^8$, and $3.2 \times 10^9$ molecules per cm$^3$, respectively, the calculated the concentrations of $H_2SO_4\cdots(CH_3)_2NH$, $CH_3CHO\cdots H_2SO_4$, and $CH_3CHO\cdots(CH_3)_2NH$ are $2.98 \times 10^{15}$ to $4.97 \times 10^5$, $7.34 \times 10^6$ to $5.14 \times 10^1$ and $2.09 \times 10^{-1}$ to $1.47 \times 10^{-2}$ molecules per cm$^3$, respectively at 200–340 K (see Table S3†). In particular, the concentrations of $H_2SO_4$ and $(CH_3)_2NH$ were $4.0 \times 10^8$ and $3.2 \times 10^9$ molecules per cm$^3$, respectively, while the corresponding concentration of the $H_2SO_4\cdots(CH_3)_2NH$ dimer was calculated to be $2.98 \times 10^{15}$ to $4.64 \times 10^8$ molecule per cm$^3$ over the 200–280 K. The larger concentration of the $H_2SO_4\cdots(CH_3)_2NH$ dimer was caused by the larger equilibrium constant at low temperatures in Table S3.† Moreover, the concentration of the $H_2SO_4\cdots(CH_3)_2NH$ complex was much higher than those of $CH_3CHO\cdots H_2SO_4$ and $CH_3CHO\cdots(CH_3)_2NH$. In addition, the peak concentration of sulfuric acid in the atmospheric boundary layer during the daytime is about $10^6$–$3 \times 10^7$ molecules per cm$^3$ and the addition of dimethylamine can stabilize clusters and reduce evaporation.[25,80] Therefore, we only considered the entrance channel $CH_3CHO + H_2SO_4\cdots(CH_3)_2NH$ in the present investigation.

The $CH_3CHO + H_2SO_4\cdots(CH_3)_2NH$ reaction occurs in one elementary step as depicted in Fig. 1, which is similar to the hydrolysis of acetaldehyde catalyzed by sulfuric acid, as well as the reaction of formaldehyde with sulfuric acid catalyzed by formic acid and other catalysts.[34,36,50,51,53,81–83] It can be seen that when the $H_2SO_4\cdots(CH_3)_2NH$ complex and $CH_3CHO$ act as reactants, the reaction occurs *via* the formation of pre-reaction complexes and then undergoes a unimolecular isomerization through these corresponding transition states responsible for the formation of the post-reaction complex. In the $CH_3CHO + H_2SO_4\cdots(CH_3)_2NH$ reaction, there is a concerted reaction mechanism where the hydrogen atom of the OH group in sulfuric acid is transferred to the oxygen atom of the carbonyl group in $CH_3CHO$ by the amino group in dimethylamine, and the oxygen atom of the S=O group in sulfuric acid is simultaneously added to the carbon atom in $CH_3CHO$, where dimethylamine acts as a catalyst; this leads to the formation of the most stable post-reaction complex (CP1), which is a nucleation precursor of secondary organic aerosols.[31] We also note that the formation of P1 is endothermic with respect to the $H_2SO_4\cdots(CH_3)_2NH$ and $CH_3CHO$ reactants and, therefore, the reverse reaction is possible.

The pre-reaction complexes ($CH_3CHO\cdots H_2SO_4\cdots(CH_3)_2NH$) have an eight-membered ring structure with two hydrogen-bonded interactions and a van der Waals interactions. As can be seen from Fig. S4,† the bond lengths of the C1–O16 bond, the N5–H3 bond and the O15–H17 bond in C1A are the same as those in C1B. From C1A and C1B to TS1A and TS1B, the C1–O16 bond length decreased from 2.731 Å to 1.846 Å and 1.848 Å, the N5–H3 bond distance increased from 1.034 Å to 1.259 Å and 1.282 Å, and the O15–H17 bond was lengthened to 1.989 Å and 1.979 Å from 1.551 Å respectively. The O15–H18 bond in sulfuric acid was lengthened to 1.967 Å from 1.565 Å, and the N5–H3 bond increased to 1.283 Å from 1.033 Å and the bond distance between the C1 atom of the aldehyde group in $CH_3CHO$ and the O17 atom of $H_2SO_4$ was shortened to 1.837 Å from 2.793 Å from C1C to TS1C. From a geometrical point of view, dimethylamine plays a crucial bridging role in the $(CH_3)_2NH$-catalyzed reaction of sulfuric acid with acetaldehyde.

The binding energies of the pre-reaction complexes (C1A, C1B, and C1C) were computed to be $-34.76$, $-34.76$ and $-35.10$ kcal mol$^{-1}$ with respect to the separate reactants. Additionally, the binding energies of the $CH_3CHO\cdots H_2SO_4\cdots(CH_3)_2NH$ complexes are also 11.60–13.76 kcal mol$^{-1}$ lower than those of the $HCHO\cdots H_2SO_4\cdots NH_3$ complexes at the M08-SO/maug-cc-pVTZ level.[81] This shows that dimethylamine has a stronger ability to form molecular clusters, compared with ammonia.

In the $CH_3CHO + H_2SO_4 + (CH_3)_2NH$ reaction, we found six different transition states (TS1A, TS1B, TS1C, TS1D, TS1E, and TS1F) as shown in Fig. S3.† The differences among them are produced by the relative orientation of the dangling OH group in sulfuric acid and the attack of $CH_3CHO$ on the $H_2SO_4\cdots(CH_3)_2NH$ complex from different directions. The six transition states are three isomers, where each isomer has two conformations (TS1A and TS1D, TS1B and TS1E, TS1C and TS1F). Additionally, the energy barriers for TS1A, TS1B, TS1C, TS1D, TS1E and TS1F were computed to be $-21.50$, $-21.14$, $-20.82$, $-18.78$, $-18.32$ and $-17.87$ kcal mol$^{-1}$, respectively, shown in Fig. S3.† The energy barriers of TS1D, TS1E, and TS1F are higher than those of TS1A, TS1B, and TS1C by about 2.04–3.63 kcal mol$^{-1}$, therefore, we did not consider TS1D, TS1E, and TS1F for kinetics calculations.

From Fig. S2,† there are three different reaction pathways and the energy barriers of the $CH_3CHO + H_2SO_4$ reaction were computed to be 0.41, 0.43 and 1.58 kcal mol$^{-1}$ for TS2A, TS2B and TS2C in the $CH_3CHO + H_2SO_4$ reaction. Therefore, the energy barriers of the $CH_3CHO + H_2SO_4 + (CH_3)_2NH$ reaction decreased by about 21.23–23.08 kcal mol$^{-1}$, as compared with the $CH_3CHO + H_2SO_4$ reaction. These results show that dimethylamine plays a remarkable catalytic role in the $CH_3CHO + H_2SO_4 + (CH_3)_2NH$ reaction. Furthermore, some similar reactions have been studied previously. For example, the energy barrier of the $HCHO + HNO_3$ reaction was reduced by 21.97 kcal mol$^{-1}$ with the assistance of $(CH_3)_2NH$.[84] The energy barrier of the reaction between $H_2SO_4$ and HCHO decreased by 16–21 kcal mol$^{-1}$ when $NH_3$ was added to the catalyst.[81] The energy barrier of the $HCHO + H_2SO_4$ reaction catalyzed by HCOOH is about 14.81 kcal mol$^{-1}$ lower than that of the $HCHO + H_2SO_4$ reaction.[53] Compared with these similar reactions, it can be seen that $(CH_3)_2NH$ has an excellent catalytic effect. Thus, the above conclusions also suggest that dimethylamine

plays a crucial catalytic role in the $CH_3CHO + H_2SO_4 + (CH_3)_2NH$ reaction, and the reaction of acetaldehyde with sulfuric acid catalyzed by $(CH_3)_2NH$ accelerates the formation of nucleation precursors in the atmosphere.

### 3.2. Kinetics

Because the temperature of the earth's atmosphere varies with the different regions, we considered the rate constants at different temperatures. Herein, we have calculated the rate constants for the three pathways of the trimolecular reaction using conventional transition state theory with Eckart tunneling in the temperature range between 200 and 298 K.

With regard to the $CH_3CHO + H_2SO_4 + (CH_3)_2NH$ reaction, we only considered $H_2SO_4\cdots(CH_3)_2NH$ and $CH_3CHO$ as reactants, and the reaction mechanism is written as follows in (R2) and (R3):

$$(CH_3)_2NH + H_2SO_4 \leftrightarrow H_2SO_4\cdots(CH_3)_2NH \quad (R2)$$

$$H_2SO_4\cdots(CH_3)_2NH + CH_3CHO \rightarrow CH_3HC(OH)OSO_3H + (CH_3)_2NH \quad (R3)$$

Thus, the total reaction rate of (R1) is computed as shown in the following eqn (1):

$$v_1 = \frac{d[CH_3HC(OH)OSO_3H]}{dt} = K_{eq1}k_1[CH_3CHO][H_2SO_4]\left[(CH_3)_2NH\right] \quad (1)$$

In the above equation, $K_{eq1}$ is the equilibrium constant of the complex $H_2SO_4\cdots(CH_3)_2NH$ relative to the reactants $H_2SO_4$ and $(CH_3)_2NH$, and $k_1$ represents the rate constant of reaction (R3). The calculated details are provided in the ESI.† The rate constant $k_1$ of the $H_2SO_4\cdots(CH_3)_2NH + CH_3CHO$ reaction was computed to be $1.55 \times 10^{-16}$ to $2.69 \times 10^{-16}$ $cm^3$ per molecules per s at 200–298 K (see Table 1). The computed result shows that the bimolecular reaction of $H_2SO_4\cdots(CH_3)_2NH$ with $CH_3CHO$ has a slightly positive temperature dependence. In addition, we also computed the bimolecular rate constant of the $CH_3CHO + H_2SO_4$ reaction.

$$CH_3CHO + H_2SO_4 \rightarrow CH_3HC(OH)OSO_3H \quad (R4)$$

The reaction rate of acetaldehyde with sulfuric acid is expressed as follows:

$$v_2 = \frac{d[CH_3HC(OH)OSO_3H]}{dt} = k_2[CH_3CHO][H_2SO_4] \quad (2)$$

The rate constant $k_2$ of the reaction was computed to be $3.88 \times 10^{-16}$ to $5.77 \times 10^{-16}$ $cm^3$ per molecule per s at 200–298 K, as shown in Table S4;† this is still a slightly positive temperature dependence.

### 3.3 Atmospheric implications

To estimate the catalytic ability of dimethylamine in the $H_2SO_4 + (CH_3)_2NH + CH_3CHO$ reaction (R1), we considered the rate ratio of $v_1/v_2$, as written in eqn (3):

$$\frac{v_1}{v_2} = \frac{K_{eq1}k_1[CH_3CHO][H_2SO_4]\left[(CH_3)_2NH\right]}{k_2[CH_3CHO][H_2SO_4]} = \frac{K_{eq1}k_1\left[(CH_3)_2NH\right]}{k_2} \quad (3)$$

The rate ratio $v_1/v_2$ depends on both the concentration of dimethylamine and temperature. When the concentration of dimethylamine is $3.2 \times 10^9$ molecules per $cm^3$, measured in a contaminated environment,[79] the values of $v_1/v_2$ are in the range $2.98 \times 10^6$ to $9.95 \times 10^0$ at 200–260 K (see Table S5†). These results show that dimethylamine makes a significant contribution in the reaction of acetaldehyde with sulfuric acid at low temperatures. The results also indicate the strong catalytic ability of dimethylamine in the $H_2SO_4 + (CH_3)_2NH + CH_3CHO$ reaction.

The main sink pathway of acetaldehyde is its reaction with OH with an atmospheric lifetime of about one day.[37,85] To further investigate the important atmospheric contribution of the $H_2SO_4 + (CH_3)_2NH + CH_3CHO$ reaction, we compared the $H_2SO_4 + (CH_3)_2NH + CH_3CHO$ reaction with $CH_3CHO + OH$. The rate ratio is expressed in eqn (4):

$$\frac{v_1}{v_{CH_3CHO+OH}} = \frac{K_{eq1}k_1[CH_3CHO][H_2SO_4]\left[(CH_3)_2NH\right]}{k_{CH_3CHO+OH}[CH_3CHO][OH]} = \frac{K_{eq1}k_1[H_2SO_4]\left[(CH_3)_2NH\right]}{k_{CH_3CHO+OH}[OH]} \quad (4)$$

where $k_{CH_3CHO+OH}$ is the experimental rate constant of the $CH_3CHO + OH$ reaction at different temperatures.[86]

From eqn (4), it can be seen that $v_1/v_{CH_3CHO+OH}$ is related to the concentrations of sulfuric acid, dimethylamine, and OH. Atmospheric sulfuric acid concentrations are in the range of $10^4$ to $4.0 \times 10^8$ molecules per $cm^3$ in different areas.[87–89] The concentration of $(CH_3)_2NH$ is often $3.2 \times 10^9$ molecules per $cm^3$.[79] However, the concentration of OH is remarkably varied during the daytime and nighttime, with values in the range of $10^4$–$10^6$ molecules per $cm^3$.[90,91] When the concentration of $(CH_3)_2NH$ is $3.2 \times 10^9$ molecules per $cm^3$ and the concentration of sulfuric acid is $10^6$, $10^7$, $4.0 \times 10^8$ and $5.1 \times 10^9$ molecules per $cm^3$,[92] the values of $v_1/v_{CH_3CHO+OH}$ at the different concentrations of OH are as listed in Tables S6–S9† at 200–298 K. When $[(CH_3)_2NH]$ and $[H_2SO_4]$ are $3.2 \times 10^9$, and $1.0 \times 10^6$ molecules per $cm^3$, respectively, the rate ratio $v_1/v_{CH_3CHO+OH}$ as the function of OH concentration is shown in Fig. 2 at 200–298 K. When [OH], $[CH_3CHO]$,[32,34] $[H_2SO_4]$, and $[(CH_3)_2NH]$ are $1.0 \times 10^6$, $1.12 \times 10^{12}$, $1.0 \times 10^6$, and $3.2 \times 10^9$ molecules per $cm^3$, respectively, the rate ratio of $v_1/v_{CH_3CHO+OH}$ is 3.67 at 220 K (listed in Table S6†); this shows that even if the OH concentration is very high during the daytime, the $H_2SO_4 + (CH_3)_2NH + CH_3CHO$ reaction can make some contribution to the sink for $CH_3CHO$. Furthermore, when the OH concentration is further decreased to $1.0 \times 10^4$ molecules per $cm^3$ during the night, the three-molecule reaction of acetaldehyde with sulfuric acid catalyzed by dimethylamine can compete well with the $CH_3CHO + OH$ reaction with the concentrations of $H_2SO_4$ ($1.0 \times 10^6$ molecules per $cm^3$) and $(CH_3)_2NH$ ($3.2 \times 10^9$ molecules per $cm^3$) below 240

 

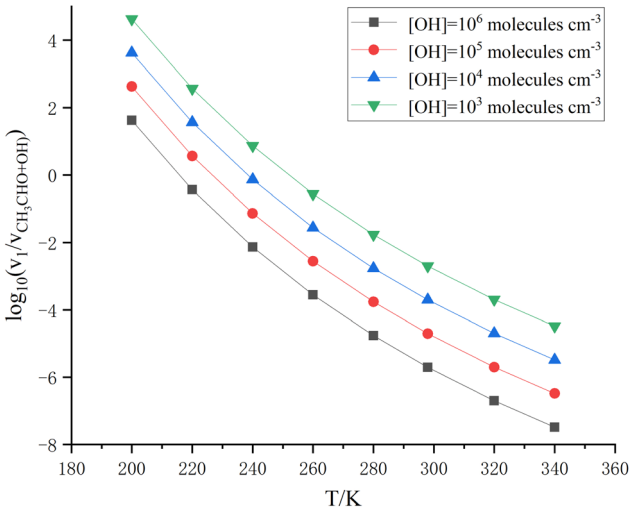


Fig. 2 Rate ratio $v_1/v_{CH_3CHO+OH}$ at $[H_2SO_4] = 1.0 \times 10^6$ molecules per $cm^3$, and $[(CH_3)_2NH] = 3.2 \times 10^9$ molecules per $cm^3$ at different temperatures and different OH concentrations.

K in Table S6;† this shows that the $H_2SO_4$ + $(CH_3)_2NH$ + $CH_3CHO$ reaction contributes significantly to the formation of organosulfates and the sink for acetaldehyde. In particular, previous studies have shown that carbonyl compounds can promote the formation of secondary organic aerosols through oxidation, hydration, and other reactions.[39,93,94] Therefore, the $H_2SO_4$ + $(CH_3)_2NH$ + $CH_3CHO$ reaction may be expected to be like the other reactions of other aldehydes with sulfuric acid catalyzed by dimethylamine, responsible for the formation of organosulfates in the gas phase reaction of the atmosphere.

We also compared the $H_2SO_4$ + $(CH_3)_2NH$ + $CH_3CHO$ reaction with the $H_2SO_4$ + OH reaction. The rate ratio is given in eqn (5):

$$\frac{v_1}{v_{H_2SO_4+OH}} = \frac{K_{eq1}k_1[CH_3CHO][H_2SO_4][(CH_3)_2NH]}{k_{H_2SO_4+OH}[H_2SO_4][OH]} = \frac{K_{eq1}k_1[CH_3CHO][(CH_3)_2NH]}{k_{H_2SO_4+OH}[OH]} \quad (5)$$

where $k_{H_2SO_4+OH}$ is the rate constant of the $H_2SO_4$ + OH reaction, which has been reported in the literature.[95] When $[CH_3CHO] = 1.12 \times 10^{12}$ molecules per $cm^3$, $[(CH_3)_2NH] = 3.20 \times 10^9$ molecules per $cm^3$, $[OH] = 10^3$, $10^4$, $10^5$, and $10^6$ molecules per $cm^3$ respectively, the values of the rate ratio of $v_1/v_{H_2SO_4+OH}$ are $1.10 \times 10^{15}$ to $2.83 \times 10^4$ at 200–298 K (see Table S10†). Therefore, the calculated results show that the $H_2SO_4$ + $(CH_3)_2NH$ + $CH_3CHO$ reaction can compete well with the $H_2SO_4$ + OH reaction.

The atmospheric lifetimes of sulfuric acid determined by heterogeneous processes are estimated to be approximately $10^2$ s in polluted air and $10^4$ s in clean air.[96] In the $H_2SO_4$ + $(CH_3)_2NH$ + $CH_3CHO$ reaction, the corresponding atmospheric lifetime of sulfuric acid was estimated mainly based on the concentrations of acetaldehyde and dimethylamine and the corresponding reaction rates as listed in Table S11.† In previous studies, acetaldehyde concentrations of 0.10 ppb–45.60 ppb were measured in some rural areas and in ambient air.[97–99] With $[(CH_3)_2NH] = 3.2 \times 10^9$ molecules per $cm^3$ and $[CH_3CHO] = 2.46 \times 10^9$ and $1.12 \times 10^{12}$ molecules per $cm^3$, respectively, the atmospheric lifetimes of $H_2SO_4$ were calculated to be about $3.52 \times 10^{-1}$ to $1.37 \times 10^7$ and $7.74 \times 10^{-4}$ to $3.01 \times 10^4$ s at 200–298 K (see Tables S11 and S12†). The atmospheric lifetime of sulfuric acid was $3.52 \times 10^{-1}$ and $7.74 \times 10^{-4}$ s at 200 K, when the concentration of dimethylamine was $3.2 \times 10^9$ molecules per $cm^3$ and the concentration of acetaldehyde was $2.46 \times 10^9$ and $1.12 \times 10^{12}$ molecules per $cm^3$, respectively. Therefore, the $H_2SO_4$ + $(CH_3)_2NH$ + $CH_3CHO$ reaction only makes a limited contribution to the sulfuric acid sinks in the atmosphere.

## 4. Conclusions

In this article, the reaction mechanisms and kinetics of the trimolecular reaction of sulfuric acid with acetaldehyde catalyzed by dimethylamine have been investigated using high-level quantum chemical methods and conventional transition state theory with Eckart tunneling. The calculated results show that dimethylamine has a strong catalytic effect in the $H_2SO_4$ + $(CH_3)_2NH$ + $CH_3CHO$ reaction responsible for the formation of organosulfates in the gas phase of the atmosphere, which was previously considered *via* heterogeneous processes. The calculated kinetic results reveal that the $H_2SO_4$ + $(CH_3)_2NH$ + $CH_3CHO$ reaction can be an important sink for acetaldehyde in the atmospheric gas-phase reactions below 240 K when the OH concentration is about $10^4$ molecules $cm^{-3}$ and the $H_2SO_4$ concentration is about $1.0 \times 10^6$ molecules per $cm^3$. Moreover, the $H_2SO_4$ + $(CH_3)_2NH$ + $CH_3CHO$ reaction makes only a limited contribution to the sink for sulfuric acid. The present findings show that organosulfates can be formed *via* the reaction of $CH_3CHO$ with sulfuric acid catalyzed by dimethylamine, which provides a new insight into the initial nucleation process for sulfuric acid, amines, and aldehydes.

## Conflicts of interest

The authors declare no competing financial interests.

## Acknowledgements

This work was supported in part by the National Natural Science Foundation of China and (4211001056, 41775125 and 91961123), by Guizhou Provincial Science and Technology Projects, China (CXTD [2022]001), and by the Science and Technology Foundation of Guizhou Provincial Department of Education, China (No. KY [2021]014 and KY[2021]107).

## References

1 J. H. Kroll and J. H. Seinfeld, Chemistry of secondary organic aerosol: Formation and evolution of low-volatility organics in the atmosphere, *Atmos. Environ.*, 2008, **42**, 3593–3624.
2 P. J. Ziemann and R. Atkinson, Kinetics, products, and mechanisms of secondary organic aerosol formation, *Chem. Soc. Rev.*, 2012, **41**, 6582–6605.

3 J. Wang, J. Ye, Q. Zhang, J. Zhao, Y. Wu, J. Li, D. Liu, W. Li, Y. Zhang, C. Wu, C. Xie, Y. Qin, Y. Lei, X. Huang, J. Guo, P. Liu, P. Fu, Y. Li, H. C. Lee, H. Choi, J. Zhang, H. Liao, M. Chen, Y. Sun, X. Ge, S. T. Martin and D. J. Jacob, Aqueous production of secondary organic aerosol from fossil-fuel emissions in winter Beijing haze, *Proc. Natl. Acad. Sci. U. S. A.*, 2021, **118**, e2022179118.

4 S. M. Charan, Y. Huang and J. H. Seinfeld, Computational Simulation of Secondary Organic Aerosol Formation in Laboratory Chambers, *Chem. Rev.*, 2019, **119**, 11912–11944.

5 A. Akherati, Y. He, M. M. Coggon, A. R. Koss, A. L. Hodshire, K. Sekimoto, C. Warneke, J. de Gouw, L. Yee, J. H. Seinfeld, T. B. Onasch, S. C. Herndon, W. B. Knighton, C. D. Cappa, M. J. Kleeman, C. Y. Lim, J. H. Kroll, J. R. Pierce and S. H. Jathar, Oxygenated Aromatic Compounds are Important Precursors of Secondary Organic Aerosol in Biomass-Burning Emissions, *Environ. Sci. Technol.*, 2020, **54**, 8568–8579.

6 Y. Zhang, Y. Chen, Z. Lei, N. E. Olson, M. Riva, A. R. Koss, Z. Zhang, A. Gold, J. T. Jayne, D. R. Worsnop, T. B. Onasch, J. H. Kroll, B. J. Turpin, A. P. Ault and J. D. Surratt, Joint Impacts of Acidity and Viscosity on the Formation of Secondary Organic Aerosol from Isoprene Epoxydiols (IEPOX) in Phase Separated Particles, *ACS Earth Space Chem.*, 2019, **3**, 2646–2658.

7 P. H. Chowdhury, Q. He, R. Carmieli, C. Li, Y. Rudich and M. Pardo, Connecting the Oxidative Potential of Secondary Organic Aerosols with Reactive Oxygen Species in Exposed Lung Cells, *Environ. Sci. Technol.*, 2019, **53**, 13949–13958.

8 I. M. Al-Naiema, J. H. Offenberg, C. J. Madler, M. Lewandowski, J. Kettler, T. Fang and E. A. Stone, Secondary organic aerosols from aromatic hydrocarbons and their contribution to fine particulate matter in Atlanta, Georgia, *Atmos. Environ.*, 2020, **223**, 117227.

9 M. Hallquist, J. C. Wenger, U. Baltensperger, Y. Rudich, D. Simpson, M. Claeys, J. Dommen, N. M. Donahue, C. George, A. H. Goldstein, J. F. Hamilton, H. Herrmann, T. Hoffmann, Y. Iinuma, M. Jang, M. E. Jenkin, J. L. Jimenez, A. Kiendler-Scharr, W. Maenhaut, G. McFiggans, T. F. Mentel, A. Monod, A. S. H. Prévôt, J. H. Seinfeld, J. D. Surratt, R. Szmigielski and J. Wildt, The formation, properties and impact of secondary organic aerosol: current and emerging issues, *Atmos. Chem. Phys.*, 2009, **9**, 5155–5236.

10 M. Mahilang, M. K. Deb and S. Pervez, Biogenic secondary organic aerosols: A review on formation mechanism, analytical challenges and environmental impacts, *Chemosphere*, 2021, **262**, 127771.

11 G. McFiggans, T. F. Mentel, J. Wildt, I. Pullinen, S. Kang, E. Kleist, S. Schmitt, M. Springer, R. Tillmann, C. Wu, D. Zhao, M. Hallquist, C. Faxon, M. Le Breton, Å. M. Hallquist, D. Simpson, R. Bergström, M. E. Jenkin, M. Ehn, J. A. Thornton, M. R. Alfarra, T. J. Bannan, C. J. Percival, M. Priestley, D. Topping and A. Kiendler-Scharr, Secondary organic aerosol reduced by mixture of atmospheric vapours, *Nature*, 2019, **565**, 587–593.

12 J. Wei, T. Fang, C. Wong, P. S. J. Lakey, S. A. Nizkorodov and M. Shiraiwa, Superoxide Formation from Aqueous Reactions of Biogenic Secondary Organic Aerosols, *Environ. Sci. Technol.*, 2021, **55**, 260–270.

13 H. Tong, P. S. J. Lakey, A. M. Arangio, J. Socorro, F. Shen, K. Lucas, W. H. Brune, U. Pöschl and M. Shiraiwa, Reactive Oxygen Species Formed by Secondary Organic Aerosols in Water and Surrogate Lung Fluid, *Environ. Sci. Technol.*, 2018, **52**, 11642–11651.

14 J. H. Slade, A. P. Ault, A. T. Bui, J. C. Ditto, Z. Lei, A. L. Bondy, N. E. Olson, R. D. Cook, S. J. Desrochers, R. M. Harvey, M. H. Erickson, H. W. Wallace, S. L. Alvarez, J. H. Flynn, B. E. Boor, G. A. Petrucci, D. R. Gentner, R. J. Griffin and P. B. Shepson, Bouncier Particles at Night: Biogenic Secondary Organic Aerosol Chemistry and Sulfate Drive Diel Variations in the Aerosol Phase in a Mixed Forest, *Environ. Sci. Technol.*, 2019, **53**, 4977–4987.

15 Y. Li and M. Shiraiwa, Timescales of secondary organic aerosols to reach equilibrium at various temperatures and relative humidities, *Atmos. Chem. Phys.*, 2019, **19**, 5959–5971.

16 X. Qi, S. Zhu, C. Zhu, J. Hu, S. Lou, L. Xu, J. Dong and P. Cheng, Smog chamber study of the effects of NOx and $NH_3$ on the formation of secondary organic aerosols and optical properties from photo-oxidation of toluene, *Sci. Total Environ.*, 2020, **727**, 138632.

17 S.-H. Lee, H. Gordon, H. Yu, K. Lehtipalo, R. Haley, Y. Li and R. Zhang, New Particle Formation in the Atmosphere: From Molecular Clusters to Global Climate, *J. Geophys. Res.: Atmos.*, 2019, **124**, 7098–7146.

18 M. Shrivastava, C. D. Cappa, J. Fan, A. H. Goldstein, A. B. Guenther, J. L. Jimenez, C. Kuang, A. Laskin, S. T. Martin, N. L. Ng, T. Petaja, J. R. Pierce, P. J. Rasch, P. Roldin, J. H. Seinfeld, J. Shilling, J. N. Smith, J. A. Thornton, R. Volkamer, J. Wang, D. R. Worsnop, R. A. Zaveri, A. Zelenyuk and Q. Zhang, Recent advances in understanding secondary organic aerosol: Implications for global climate forcing, *Rev. Geophys.*, 2017, **55**, 509–559.

19 J. Li, Z. Liu, W. Gao, G. Tang, B. Hu, Z. Ma and Y. Wang, Insight into the formation and evolution of secondary organic aerosol in the megacity of Beijing, China, *Atmos. Environ.*, 2020, **220**, 117070.

20 M. Kulmala, J. Kontkanen, H. Junninen, K. Lehtipalo, H. E. Manninen, T. Nieminen, T. Petäjä, M. Sipilä, S. Schobesberger, P. Rantala, A. Franchin, T. Jokinen, E. Järvinen, M. Äijälä, J. Kangasluoma, J. Hakala, P. P. Aalto, P. Paasonen, J. Mikkilä, J. Vanhanen, J. Aalto, H. Hakola, U. Makkonen, T. Ruuskanen, R. L. Mauldin, J. Duplissy, H. Vehkamäki, J. Bäck, A. Kortelainen, I. Riipinen, T. Kurtén, M. V. Johnston, J. N. Smith, M. Ehn, T. F. Mentel, K. E. J. Lehtinen, A. Laaksonen, V.-M. Kerminen and D. R. Worsnop, Direct Observations of Atmospheric Aerosol Nucleation, *Science*, 2013, **339**, 943–946.

21 M. Kulmala, I. Riipinen, M. Sipilä, H. E. Manninen, T. Petäjä, H. Junninen, M. D. Maso, G. Mordas, A. Mirme, M. Vana, A. Hirsikko, L. Laakso, R. M. Harrison, I. Hanson, C. Leung, K. E. J. Lehtinen and V.-M. Kerminen, Toward

 

Direct Measurement of Atmospheric Nucleation, *Science*, 2007, **318**, 89–92.

22 N. Myllys, J. Elm, R. Halonen, T. Kurtén and H. Vehkamäki, Coupled Cluster Evaluation of the Stability of Atmospheric Acid–Base Clusters with up to 10 Molecules, *J. Phys. Chem. A*, 2016, **120**, 621–630.

23 F. Bianchi, A. P. Praplan, N. Sarnela, J. Dommen, A. Kürten, I. K. Ortega, S. Schobesberger, H. Junninen, M. Simon, J. Tröstl, T. Jokinen, M. Sipilä, A. Adamov, A. Amorim, J. Almeida, M. Breitenlechner, J. Duplissy, S. Ehrhart, R. C. Flagan, A. Franchin, J. Hakala, A. Hansel, M. Heinritzi, J. Kangasluoma, H. Keskinen, J. Kim, J. Kirkby, A. Laaksonen, M. J. Lawler, K. Lehtipalo, M. Leiminger, V. Makhmutov, S. Mathot, A. Onnela, T. Petäjä, F. Riccobono, M. P. Rissanen, L. Rondo, A. Tomé, A. Virtanen, Y. Viisanen, C. Williamson, D. Wimmer, P. M. Winkler, P. Ye, J. Curtius, M. Kulmala, D. R. Worsnop, N. M. Donahue and U. Baltensperger, Insight into Acid–Base Nucleation Experiments by Comparison of the Chemical Composition of Positive, Negative, and Neutral Clusters, *Environ. Sci. Technol.*, 2014, **48**, 13675–13684.

24 L. Yao, O. Garmash, F. Bianchi, J. Zheng, C. Yan, J. Kontkanen, H. Junninen, S. B. Mazon, M. Ehn, P. Paasonen, M. Sipilä, M. Wang, X. Wang, S. Xiao, H. Chen, Y. Lu, B. Zhang, D. Wang, Q. Fu, F. Geng, L. Li, H. Wang, L. Qiao, X. Yang, J. Chen, V.-M. Kerminen, T. Petäjä, D. R. Worsnop, M. Kulmala and L. Wang, Atmospheric new particle formation from sulfuric acid and amines in a Chinese megacity, *Science*, 2018, **361**, 278–281.

25 J. Almeida, S. Schobesberger, A. Kürten, I. K. Ortega, O. Kupiainen-Määttä, A. P. Praplan, A. Adamov, A. Amorim, F. Bianchi, M. Breitenlechner, A. David, J. Dommen, N. M. Donahue, A. Downard, E. Dunne, J. Duplissy, S. Ehrhart, R. C. Flagan, A. Franchin, R. Guida, J. Hakala, A. Hansel, M. Heinritzi, H. Henschel, T. Jokinen, H. Junninen, M. Kajos, J. Kangasluoma, H. Keskinen, A. Kupc, T. Kurtén, A. N. Kvashin, A. Laaksonen, K. Lehtipalo, M. Leiminger, J. Leppä, V. Loukonen, V. Makhmutov, S. Mathot, M. J. McGrath, T. Nieminen, T. Olenius, A. Onnela, T. Petäjä, F. Riccobono, I. Riipinen, M. Rissanen, L. Rondo, T. Ruuskanen, F. D. Santos, N. Sarnela, S. Schallhart, R. Schnitzhofer, J. H. Seinfeld, M. Simon, M. Sipilä, Y. Stozhkov, F. Stratmann, A. Tomé, J. Tröstl, G. Tsagkogeorgas, P. Vaattovaara, Y. Viisanen, A. Virtanen, A. Vrtala, P. E. Wagner, E. Weingartner, H. Wex, C. Williamson, D. Wimmer, P. Ye, T. Yli-Juuti, K. S. Carslaw, M. Kulmala, J. Curtius, U. Baltensperger, D. R. Worsnop, H. Vehkamäki and J. Kirkby, Molecular understanding of sulphuric acid–amine particle nucleation in the atmosphere, *Nature*, 2013, **502**, 359–363.

26 J. Elm, Elucidating the Limiting Steps in Sulfuric Acid–Base New Particle Formation, *J. Phys. Chem. A*, 2017, **121**, 8288–8295.

27 G. Duporté, M. Riva, J. Parshintsev, E. Heikkinen, L. M. F. Barreira, N. Myllys, L. Heikkinen, K. Hartonen, M. Kulmala, M. Ehn and M.-L. Riekkola, Chemical Characterization of Gas- and Particle-Phase Products from the Ozonolysis of α-Pinene in the Presence of Dimethylamine, *Environ. Sci. Technol.*, 2017, **51**, 5602–5610.

28 A. Kürten, T. Jokinen, M. Simon, M. Sipilä, N. Sarnela, H. Junninen, A. Adamov, J. Almeida, A. Amorim, F. Bianchi, M. Breitenlechner, J. Dommen, N. M. Donahue, J. Duplissy, S. Ehrhart, R. C. Flagan, A. Franchin, J. Hakala, A. Hansel, M. Heinritzi, M. Hutterli, J. Kangasluoma, J. Kirkby, A. Laaksonen, K. Lehtipalo, M. Leiminger, V. Makhmutov, S. Mathot, A. Onnela, T. Petäjä, A. P. Praplan, F. Riccobono, M. P. Rissanen, L. Rondo, S. Schobesberger, J. H. Seinfeld, G. Steiner, A. Tomé, J. Tröstl, P. M. Winkler, C. Williamson, D. Wimmer, P. Ye, U. Baltensperger, K. S. Carslaw, M. Kulmala, D. R. Worsnop and J. Curtius, Neutral molecular cluster formation of sulfuric acid–dimethylamine observed in real time under atmospheric conditions, *Proc. Natl. Acad. Sci.*, 2014, **111**, 15019–15024.

29 J. Elm, P. Norman and K. V. Mikkelsen, Rayleigh light scattering properties of atmospheric molecular clusters consisting of sulfuric acid and bases, *Phys. Chem. Chem. Phys.*, 2015, **17**, 15701–15709.

30 M. Jang and R. M. Kamens, Atmospheric Secondary Aerosol Formation by Heterogeneous Reactions of Aldehydes in the Presence of a Sulfuric Acid Aerosol Catalyst, *Environ. Sci. Technol.*, 2001, **35**, 4758–4766.

31 R. Zhang, A. Khalizov, L. Wang, M. Hu and W. Xu, Nucleation and Growth of Nanoparticles in the Atmosphere, *Chem. Rev.*, 2012, **112**, 1957–2011.

32 S. M. Corrêa, E. M. Martins and G. Arbilla, Formaldehyde and acetaldehyde in a high traffic street of Rio de Janeiro, Brazil, *Atmos. Environ.*, 2003, **37**, 23–29.

33 J. F. Doussin, B. Picquet-Varrault, R. Durand-Jolibois, H. Loirat and P. Carlier, A visible and FTIR spectrometric study of the nighttime chemistry of acetaldehyde and PAN under simulated atmospheric conditions, *J. Photochem. Photobiol., A*, 2003, **157**, 283–293.

34 X.-F. Tan, B. Long, D.-S. Ren, W.-J. Zhang, Z.-W. Long and E. Mitchell, Atmospheric chemistry of $CH_3CHO$: the hydrolysis of $CH_3CHO$ catalyzed by $H_2SO_4$, *Phys. Chem. Chem. Phys.*, 2018, **20**, 7701–7709.

35 Y. Cheng, S. C. Lee, Y. Huang, K. F. Ho, S. S. H. Ho, P. S. Yau, P. K. K. Louie and R. J. Zhang, Diurnal and seasonal trends of carbonyl compounds in roadside, urban, and suburban environment of Hong Kong, *Atmos. Environ.*, 2014, **89**, 43–51.

36 Z.-G. Dong, F. Xu and B. Long, The energetics and kinetics of the $CH_3CHO$ + $(CH_3)_2NH/CH_3NH_2$ reactions catalyzed by a single water molecule in the atmosphere, *Comput. Theor. Chem.*, 2018, **1140**, 7–13.

37 D. B. Millet, A. Guenther, D. A. Siegel, N. B. Nelson, H. B. Singh, J. A. de Gouw, C. Warneke, J. Williams, G. Eerdekens, V. Sinha, T. Karl, F. Flocke, E. Apel, D. D. Riemer, P. I. Palmer and M. Barkley, Global atmospheric budget of acetaldehyde: 3-D model analysis and constraints from in-situ and satellite observations, *Atmos. Chem. Phys.*, 2010, **10**, 3405–3425.

38 K. Yamada, R. Hattori, Y. Ito, H. Shibata and N. Yoshida, Carbon isotopic signatures of methanol and acetaldehyde emitted from biomass burning source, *Geophys. Res. Lett.*, 2009, **36**, L18807.

39 Z. Li, A. N. Schwier, N. Sareen and V. F. McNeill, Reactive processing of formaldehyde and acetaldehyde in aqueous aerosol mimics: surface tension depression and secondary organic products, *Atmos. Chem. Phys.*, 2011, **11**, 11617–11629.

40 H. A. Rypkema, A. Sinha and J. S. Francisco, Carboxylic Acid Catalyzed Hydration of Acetaldehyde, *J. Phys. Chem. A*, 2015, **119**, 4581–4588.

41 S. Sarkar, B. K. Oram and B. Bandyopadhyay, Ammonolysis as an important loss process of acetaldehyde in the troposphere: energetics and kinetics of water and formic acid catalyzed reactions, *Phys. Chem. Chem. Phys.*, 2019, **21**, 16170–16179.

42 L. Benning and A. Wahner, Measurements of Atmospheric Formaldehyde (HCHO) and Acetaldehyde ($CH_3CHO$) during POPCORN 1994 Using 2.4-DNPH Coated Silica Cartridges, *J. Atmos. Chem.*, 1998, **31**, 105–117.

43 J. D. Surratt, J. H. Kroll, T. E. Kleindienst, E. O. Edney, M. Claeys, A. Sorooshian, N. L. Ng, J. H. Offenberg, M. Lewandowski, M. Jaoui, R. C. Flagan and J. H. Seinfeld, Evidence for Organosulfates in Secondary Organic Aerosol, *Environ. Sci. Technol.*, 2007, **41**, 517–527.

44 J. Liggio and S.-M. Li, Organosulfate formation during the uptake of pinonaldehyde on acidic sulfate aerosols, *Geophys. Res. Lett.*, 2006, **33**, L13808.

45 M. Brüggemann, R. Xu, A. Tilgner, K. C. Kwong, A. Mutzel, H. Y. Poon, T. Otto, T. Schaefer, L. Poulain, M. N. Chan and H. Herrmann, Organosulfates in Ambient Aerosol: State of Knowledge and Future Research Directions on Formation, Abundance, Fate, and Importance, *Environ. Sci. Technol.*, 2020, **54**, 3767–3782.

46 Y. Zhao and D. G. Truhlar, The M06 suite of density functionals for main group thermochemistry, thermochemical kinetics, noncovalent interactions, excited states, and transition elements: two new functionals and systematic testing of four M06-class functionals and 12 other functionals, *Theor. Chem. Acc.*, 2008, **120**, 215–241.

47 B. J. Lynch, Y. Zhao and D. G. Truhlar, Effectiveness of Diffuse Basis Functions for Calculating Relative Energies by Density Functional Theory, *J. Phys. Chem. A*, 2003, **107**, 1384–1388.

48 J. Elm, M. Bilde and K. V. Mikkelsen, Assessment of Density Functional Theory in Predicting Structures and Free Energies of Reaction of Atmospheric Prenucleation Clusters, *J. Chem. Theory Comput.*, 2012, **8**, 2071–2077.

49 B. Long, X.-F. Tan, C.-R. Chang, W.-X. Zhao, Z.-W. Long, D.-S. Ren and W.-J. Zhang, Theoretical Studies on Gas-Phase Reactions of Sulfuric Acid Catalyzed Hydrolysis of Formaldehyde and Formaldehyde with Sulfuric Acid and $H_2SO_4\cdots H_2O$ Complex, *J. Phys. Chem. A*, 2013, **117**, 5106–5116.

50 F.-Y. Liu, X.-F. Tan, Z.-W. Long, B. Long and W.-J. Zhang, New insights in atmospheric acid-catalyzed gas phase hydrolysis of formaldehyde: a theoretical study, *RSC Adv.*, 2015, **5**, 32941–32949.

51 L. Zhang and B. Long, Hydrolysis of Formyl Fluoride Catalyzed by Sulfuric Acid and Formic Acid in the Atmosphere, *ACS Omega*, 2019, **4**, 18996–19004.

52 Z.-G. Dong, F. Xu, E. Mitchell and B. Long, Trifluoroacetaldehyde aminolysis catalyzed by a single water molecule: An important sink pathway for trifluoroacetaldehyde and a potential pathway for secondary organic aerosol growth, *Atmos. Environ.*, 2021, **249**, 118242.

53 J.-Y. Liu, Z.-W. Long, E. Mitchell and B. Long, New Mechanistic Pathways for the Reactions of Formaldehyde with Formic Acid Catalyzed by Sulfuric Acid and Formaldehyde with Sulfuric Acid Catalyzed by Formic Acid: Formation of Potential Secondary Organic Aerosol Precursors, *ACS Earth Space Chem.*, 2021, **5**, 1363–1372.

54 R. Seeger and J. A. Pople, Self-consistent molecular orbital methods. XVIII. Constraints and stability in Hartree–Fock theory, *J. Chem. Phys.*, 1977, **66**, 3045–3050.

55 R. Bauernschmitt and R. Ahlrichs, Stability analysis for solutions of the closed shell Kohn–Sham equation, *J. Chem. Phys.*, 1996, **104**, 9047–9052.

56 K. Fukui, The path of chemical reactions - the IRC approach, *Acc. Chem. Res.*, 1981, **14**, 363–368.

57 C. Gonzalez and H. B. Schlegel, Reaction path following in mass-weighted internal coordinates, *J. Phys. Chem.*, 1990, **94**, 5523–5527.

58 B. Long, J. L. Bao and D. G. Truhlar, Kinetics of the Strongly Correlated $CH_3O + O_2$ Reaction: The Importance of Quadruple Excitations in Atmospheric and Combustion Chemistry, *J. Am. Chem. Soc.*, 2019, **141**, 611–617.

59 Y. Xia, B. Long, S. Lin, C. Teng, J. L. Bao and D. G. Truhlar, Large Pressure Effects Caused by Internal Rotation in the s-cis-syn-Acrolein Stabilized Criegee Intermediate at Tropospheric Temperature and Pressure, *J. Am. Chem. Soc.*, 2022, **144**, 4828–4838.

60 J. M. L. Martin and M. K. Kesharwani, Assessment of CCSD(T)-F12 Approximations and Basis Sets for Harmonic Vibrational Frequencies, *J. Chem. Theory Comput.*, 2014, **10**, 2085–2090.

61 G. Knizia, T. B. Adler and H.-J. Werner, Simplified CCSD(T)-F12 methods: Theory and benchmarks, *J. Chem. Phys.*, 2009, **130**, 054104.

62 E. Papajak and D. G. Truhlar, Convergent Partially Augmented Basis Sets for Post-Hartree-Fock Calculations of Molecular Properties and Reaction Barrier Heights, *J. Chem. Theory Comput.*, 2011, **7**, 10–18.

63 T. J. Lee and P. R. Taylor, A diagnostic for determining the quality of single-reference electron correlation methods, *Int. J. Quantum Chem.*, 1989, **36**, 199–207.

64 H. Eyring, The Activated Complex in Chemical Reactions, *J. Chem. Phys.*, 1935, **3**, 107–115.

65 M. G. Evans and M. Polanyi, Some applications of the transition state method to the calculation of reaction velocities, especially in solution, *Trans. Faraday Soc.*, 1935, **31**, 875–894.

66 D. G. Truhlar, B. C. Garrett and S. J. Klippenstein, Current Status of Transition-State Theory, *J. Phys. Chem.*, 1996, **100**, 12771–12800.

67 C. Eckart, The Penetration of a Potential Barrier by Electrons, *Phys. Rev.*, 1930, **35**, 1303–1309.

68 M. J. Frisch, G. W. Trucks, H. B. Schlegel, G. E. Scuseria, M. A. Robb, J. R. Cheeseman, G. Scalmani, V. Barone, G. A. Petersson, H. Nakatsuji, X. Li, M. Caricato, A. V. Marenich, J. Bloino, B. G. Janesko, R. Gomperts, B. Mennucci, H. P. Hratchian, J. V. Ortiz, A. F. Izmaylov, J. L. Sonnenberg, D. Williams-Young, F. Ding, F. Lipparini, F. Egidi, J. Goings, B. Peng, A. Petrone, T. Henderson, D. Ranasinghe, V. G. Zakrzewski, J. Gao, N. Rega, G. Zheng, W. Liang, M. Hada, M. Ehara, K. Toyota, R. Fukuda, J. Hasegawa, M. Ishida, T. Nakajima, Y. Honda, O. Kitao, H. Nakai, T. Vreven, K. Throssell, J. A. Montgomery, Jr., J. E. Peralta, F. Ogliaro, M. J. Bearpark, J. J. Heyd, E. N. Brothers, K. N. Kudin, V. N. Staroverov, T. A. Keith, R. Kobayashi, J. Normand, K. Raghavachari, A. P. Rendell, J. C. Burant, S. S. Iyengar, J. Tomasi, M. Cossi, J. M. Millam, M. Klene, C. Adamo, R. Cammi, J. W. Ochterski, R. L. Martin, K. Morokuma, O. Farkas, J. B. Foresman, and D. J. Fox, *Gaussian 16, Revision A.03*, Gaussian, Inc., Wallingford CT, 2016.

69 H. J. Werner, P. J. Knowles, G. Knizia, F. R. Manby, M. Schütz, P. Celani, W. Györffy, D. Kats, T. Korona, R. Lindh, A. Mitrushenkov, G. Rauhut, K. R. Shamasundar, T. B. Adler, R. D. Amos, S. J. Bennie, A. Bernhardsson, A. Berning, D. L. Cooper, M. J. O. Deegan, A. J. Dobbyn, F. Eckert, E. Goll, C. Hampel, A. Hesselmann, G. Hetzer, T. Hrenar, G. Jansen, C. Köppl, S. J. R. Lee, Y. Liu, A. W. Lloyd, Q. Ma, R. A. Mata, A. J. May, S. J. McNicholas, W. Meyer, T. F. Miller III, M. E. Mura, A. Nicklaß, D. P. O'Neill, P. Palmieri, D. Peng, K. Pflüger, R. Pitzer, M. Reiher, T. Shiozaki, H. Stoll, A. J. Stone, R. Tarroni, T. Thorsteinsson, M. Wang and M. Welborn, *MOLPRO 2019.2, a Package of Ab Initio Programs*; Cardiff, U.K. 2018.

70 W. Duncan, R. Bell and T. Truong, TheRate: Program for ab initio direct dynamics calculations of thermal and vibrational-state-selected rate constants, *J. Comput. Chem.*, 1998, **19**, 1039–1052.

71 F. T. Smith, Three-body collision rates in atomic recombination reactions, *Discuss. Faraday Soc.*, 1962, **33**, 183–188.

72 R. T Pack, R. B. Walker and B. K. Kendrick, Three-body collision contributions to recombination and collision-induced dissociation. I. Cross sections, *J. Chem. Phys.*, 1998, **109**, 6701–6713.

73 P. A. Whitlock, J. T. Muckerman and R. E. Roberts, Classical mechanics of recombination via the resonance complex mechanism: H + H + M → $H_2$ + M for M = H, $H_2$, He, and Ar, *J. Chem. Phys.*, 1974, **60**, 3658–3673.

74 J. Pérez-Ríos, S. Ragole, J. Wang and C. H. Greene, Comparison of classical and quantal calculations of helium three-body recombination, *J. Chem. Phys.*, 2014, **140**, 044307.

75 J. Elm, M. Bilde and K. V. Mikkelsen, Influence of Nucleation Precursors on the Reaction Kinetics of Methanol with the OH Radical, *J. Phys. Chem. A*, 2013, **117**, 6695–6701.

76 P. Sebastianelli, P. M. Cometto and R. G. Pereyra, Systematic Characterization of Gas Phase Binary Pre-Nucleation Complexes Containing $H_2SO_4$ + X, [ X = $NH_3$, $(CH_3)NH_2$, $(CH_3)_2NH$, $(CH_3)_3N$, $H_2O$, $(CH_3)OH$, $(CH_3)_2O$, HF, $CH_3F$, $PH_3$, $(CH_3)PH_2$, $(CH_3)_2PH$, $(CH_3)_3P$, $H_2S$, $(CH_3)SH$, $(CH_3)_2S$, HCl, $(CH_3)Cl$)]. A Computational Study, *J. Phys. Chem. A*, 2018, **122**, 2116–2128.

77 H. R. Leverentz, J. I. Siepmann, D. G. Truhlar, V. Loukonen and H. Vehkamäki, Energetics of Atmospherically Implicated Clusters Made of Sulfuric Acid, Ammonia and Dimethyl Amine, *J. Phys. Chem. A*, 2013, **117**, 3819–3825.

78 Z. B. Wang, M. Hu, D. Mogensen, D. L. Yue, J. Zheng, R. Y. Zhang, Y. Liu, B. Yuan, X. Li, M. Shao, L. Zhou, Z. J. Wu, A. Wiedensohler and M. Boy, The simulations of sulfuric acid concentration and new particle formation in an urban atmosphere in China, *Atmos. Chem. Phys.*, 2013, **13**, 11157–11167.

79 X. Ge, A. Wexler and S. Clegg, Atmospheric amines–Part I. A review, *Atmos. Environ.*, 2011, **45**, 524–546.

80 J. Kirkby, J. Curtius, J. Almeida, E. Dunne, J. Duplissy, S. Ehrhart, A. Franchin, S. Gagné, L. Ickes, A. Kürten, A. Kupc, A. Metzger, F. Riccobono, L. Rondo, S. Schobesberger, G. Tsagkogeorgas, D. Wimmer, A. Amorim, F. Bianchi, M. Breitenlechner, A. David, J. Dommen, A. Downard, M. Ehn, R. C. Flagan, S. Haider, A. Hansel, D. Hauser, W. Jud, H. Junninen, F. Kreissl, A. Kvashin, A. Laaksonen, K. Lehtipalo, J. Lima, E. R. Lovejoy, V. Makhmutov, S. Mathot, J. Mikkilä, P. Minginette, S. Mogo, T. Nieminen, A. Onnela, P. Pereira, T. Petäjä, R. Schnitzhofer, J. H. Seinfeld, M. Sipilä, Y. Stozhkov, F. Stratmann, A. Tomé, J. Vanhanen, Y. Viisanen, A. Vrtala, P. E. Wagner, H. Walther, E. Weingartner, H. Wex, P. M. Winkler, K. S. Carslaw, D. R. Worsnop, U. Baltensperger and M. Kulmala, Role of sulphuric acid, ammonia and galactic cosmic rays in atmospheric aerosol nucleation, *Nature*, 2011, **476**, 429–433.

81 X.-F. Tan, L. Zhang and B. Long, New mechanistic pathways for the formation of organosulfates catalyzed by ammonia and carbinolamine formation catalyzed by sulfuric acid in the atmosphere, *Phys. Chem. Chem. Phys.*, 2020, **22**, 8800–8807.

82 F. Xu, X.-F. Tan, Z.-G. Dong, D.-S. Ren and B. Long, Hydrolysis of ketene catalysed by nitric acid and water in the atmosphere, *Environ. Chem.*, 2020, **17**, 457–467.

83 N. Lin, Z.-W. Long and B. Long, Important Routes for Methanediol Formation by Formaldehyde Hydrolysis Catalyzed by Iodic Acid and for the Contribution to an Iodic Acid Sink by the Reaction of Formaldehyde with Iodic Acid Catalyzed by Atmospheric Water, *ACS Earth Space Chem.*, 2022, **6**, 1890–1898.

84 G.-B. Li, S.-H. Cai and B. Long, New reactions for formation of organic nitrate in the atmosphere, *ACS Omega*, 2022, **7**, 39671–39679.

85 B. Long, Y. Xia and D. G. Truhlar, Quantitative Kinetics of $HO_2$ Reactions with Aldehydes in the Atmosphere: High-Order Dynamic Correlation, Anharmonicity, and Falloff Effects Are All Important, *J. Am. Chem. Soc.*, 2022, **144**, 19910–19920.

86 R. Atkinson, D. L. Baulch, R. A. Cox, J. N. Crowley, R. F. Hampson, R. G. Hynes, M. E. Jenkin, M. J. Rossi, J. Troe and I. Subcommittee, Evaluated kinetic and photochemical data for atmospheric chemistry: Volume II – gas phase reactions of organic species, *Atmos. Chem. Phys.*, 2006, **6**, 3625–4055.

87 F. L. Eisele and D. J. Tanner, Measurement of the gas phase concentration of $H_2SO_4$ and methane sulfonic acid and estimates of $H_2SO_4$ production and loss in the atmosphere, *J. Geophys. Res.: Atmos.*, 1993, **98**, 9001–9010.

88 T. Petäjä, I. R. L. Mauldin, E. Kosciuch, J. McGrath, T. Nieminen, P. Paasonen, M. Boy, A. Adamov, T. Kotiaho and M. Kulmala, Sulfuric acid and OH concentrations in a boreal forest site, *Atmos. Chem. Phys.*, 2009, **9**, 7435–7448.

89 S. Mikkonen, S. Romakkaniemi, J. N. Smith, H. Korhonen, T. Petäjä, C. Plass-Duelmer, M. Boy, P. H. McMurry, K. E. J. Lehtinen, J. Joutsensaari, A. Hamed, R. L. Mauldin Iii, W. Birmili, G. Spindler, F. Arnold, M. Kulmala and A. Laaksonen, A statistical proxy for sulphuric acid concentration, *Atmos. Chem. Phys.*, 2011, **11**, 11319–11334.

90 G. P. Brasseur and S. Solomon, *Aeronomy of the Middle Atmosphere: Chemistry and Physics of the Stratosphere and Mesosphere*, Springer Netherlands, 2005.

91 M. A. H. Khan, M. J. Ashfold, G. Nickless, D. Martin, L. A. Watson, P. D. Hamer, R. P. Wayne, C. E. Canosa-Mas and D. E. Shallcross, Night-time $NO_3$ and OH radical concentrations in the United Kingdom inferred from hydrocarbon measurements, *Atmos. Sci. Lett.*, 2008, **9**, 140–146.

92 M. Torrent-Sucarrat, J. S. Francisco and J. M. Anglada, Sulfuric Acid as Autocatalyst in the Formation of Sulfuric Acid, *J. Am. Chem. Soc.*, 2012, **134**, 20632–20644.

93 M. M. Galloway, M. H. Powelson, N. Sedehi, S. E. Wood, K. D. Millage, J. A. Kononenko, A. D. Rynaski and D. O. De Haan, Secondary Organic Aerosol Formation during Evaporation of Droplets Containing Atmospheric Aldehydes, Amines, and Ammonium Sulfate, *Environ. Sci. Technol.*, 2014, **48**, 14417–14425.

94 A. A. Rodriguez, A. de Loera, M. H. Powelson, M. M. Galloway and D. O. De Haan, Formaldehyde and Acetaldehyde Increase Aqueous-Phase Production of Imidazoles in Methylglyoxal/Amine Mixtures: Quantifying a Secondary Organic Aerosol Formation Mechanism, *Environ. Sci. Technol. Lett.*, 2017, **4**, 234–239.

95 J. M. Anglada, S. Olivella and A. Solé, Hydrogen Transfer between Sulfuric Acid and Hydroxyl Radical in the Gas Phase: Competition among Hydrogen Atom Transfer, Proton-Coupled Electron-Transfer, and Double Proton Transfer, *J. Phys. Chem. A*, 2006, **110**, 1982–1990.

96 M. Dal Maso, M. Kulmala, K. E. J. Lehtinen, J. M. Mäkelä, P. Aalto and C. D. O'Dowd, Condensation and coagulation sinks and formation of nucleation mode particles in coastal and boreal forest boundary layers, *J. Geophys. Res.*, 2002, **107**, 8097–8107.

97 J. Slemr, W. Junkermann and A. Volz-Thomas, Temporal variations in formaldehyde, acetaldehyde and acetone and budget of formaldehyde at a rural site in Southern Germany, *Atmos. Environ.*, 1996, **30**, 3667–3676.

98 Y.-N. Lee, X. Zhou and K. Hallock, Atmospheric carbonyl compounds at a rural southeastern United States site, *J. Geophys. Res.: Atmos.*, 1995, **100**, 25933–25944.

99 S. M. Corrêa, E. M. Martins and G. Arbilla, Formaldehyde and acetaldehyde in a high traffic street of Rio de Janeiro, Brazil, *Atmos. Environ.*, 2003, **37**, 23–29.